THE ASTROPHYSICAL JOURNAL, 203:132–142, 1976 January 1

INTERSTELLAR H_2: THE POPULATION OF EXCITED ROTATIONAL STATES AND THE INFRARED RESPONSE TO ULTRAVIOLET RADIATION

J. H. BLACK AND A. DALGARNO
Center for Astrophysics, Harvard College Observatory and Smithsonian Astrophysical Observatory
Received 1975 March 10

ABSTRACT

Molecular hydrogen in interstellar clouds absorbs ultraviolet radiation in lines of the Lyman and Werner systems. The subsequent fluorescence leads to dissociation or to the population of excited rotational-vibrational levels of the ground electronic state. The rotational-vibrational levels decay by means of quadrupole transitions which result in the emission of infrared photons and populate excited rotational levels of the lowest vibrational state. An additional input into the cascade is provided by the formation of molecules on grain surfaces. A concise tabular description of the rotation-vibration cascade is presented. Calculations of the infrared emission spectrum of H_2 are given for an illustrative cloud model which includes the processes of fluorescence and hot molecule formation. In favorable circumstances, some of the infrared lines may have detectable intensities. Due to the distribution of lines, it may prove possible to detect interstellar H_2 using narrow-band filter photometry at a wavelength of 2.4 μ.

Subject headings: atomic and molecular processes — infrared — interstellar matter — molecules, interstellar

I. INTRODUCTION

Recent ultraviolet observations of interstellar molecular hydrogen indicate not only that it is abundant in the diffuse interstellar clouds (Carruthers 1970; Smith 1973; Spitzer *et al.* 1973), but also that its excited rotational states are populated to a much greater extent than would be expected in thermal equilibrium at the inferred kinetic temperatures of 80–100 K (Spitzer *et al.* 1973; Spitzer and Cochran 1973; Spitzer *et al.* 1974). Theoretical models of such molecular clouds must treat simultaneously the balance between formation and dissociation of H_2, the radiative transfer problem for the dissociating photons, and the statistical equilibrium describing the populations of all the rotation-vibration levels of the ground electronic state. Such models then predict the emission spectrum of H_2 in the infrared. Gould and Harwit (1963) suggested that H_2 exposed to ultraviolet radiation might be observable through emission in rotation-vibration lines in the near-infrared—a suggestion which was acted upon by Werner and Harwit (1968) and by Gull and Harwit (1971), who searched for several lines of the 3–0 band in a few locations without positive results. Dalgarno and Wright (1972) have discussed the emissivities in pure rotational transitions of H_2 and HD to be expected from molecules with rotational levels thermalized at relatively low temperatures.

The present study includes a general discussion of the physical processes which govern the populations of rotation-vibration levels of H_2 in the interstellar gas and provides a convenient numerical description of the rotation-vibration cascade in tabular form. The results of detailed model calculations are used to illustrate the nature of the infrared emission spectrum of interstellar H_2. It is also suggested that the distribution of lines in the fundamental band around 2.4 μ wavelength may permit the observation of H_2 through narrow-band filter photometry without the need for a high-resolution spectrometer to search for individual lines. The actual construction of models of clouds of H_2 and the application of the theory to other astronomical phenomena will be presented in subsequent papers.

II. PHYSICAL PROCESSES

a) The Rotation-Vibration Cascade

The abundance of H_2 in interstellar clouds can usually be understood as the result of an equilibrium between formation on grain surfaces and dissociation by ultraviolet photons and ionization by cosmic rays and X-rays (Hollenbach *et al.* 1971; Solomon and Werner 1971). In regions which are not entirely opaque to ultraviolet radiation of wavelengths between 912 and 1108 Å, the dominant destruction process is the absorption of a photon in one of the Lyman or Werner system lines followed by fluorescence to the vibrational continuum of the ground electronic state, thus resulting in two separated hydrogen atoms. This mechanism was suggested originally by Solomon (see Field *et al.* 1966) and discussed quantitatively by Stecher and Williams (1967), by Nishimura and Takayanagi (1969), and by Dalgarno and Stephens (1970). The fraction of ultraviolet absorptions by H_2 which lead ultimately to dissociation depends upon the nature of the radiation field and varies as a function of depth as

lines become optically thick and shorter-wavelength photons are attenuated more efficiently by grains than are those of longer wavelengths. When the absorptions in the Werner system (which contribute negligibly to dissociation) are included, the fraction of absorptions leading to dissociation ranges roughly from 0.10 to 0.25 for typical interstellar radiation fields. The remainder of the absorptions result in the population of various rotation-vibration levels of the ground state. These excited molecules decay by means of radiative transitions which are dipole-forbidden since H_2 is a homonuclear molecule and has no permanent dipole moment. At the temperatures and densities of interstellar clouds, only the lower rotational levels of the lowest ($v'' = 0$) vibrational state are affected by inelastic collisions. Thus the cascade through excited rotation-vibration states is determined entirely by the transition probabilities of the quadrupole rotational and rotation-vibration transitions.

If R is the internuclear distance, $X_{vJ}(R)$ is the nuclear rotation-vibration wave function, and E_{vJ} is the corresponding eigenvalue, then the probability $A(v'J', v''J'')$ of a spontaneous radiative transition from an upper level with vibrational and rotational quantum numbers v' and J', respectively, to a lower level $v''J''$ with the emission of an electric quadrupole photon is given in s^{-1} by

$$A(v'J', v''J'') = 1.4258 \times 10^4 (E_{v'J'} - E_{v''J''})^5 |\langle X_{v'J'}|Q(R)|X_{v''J''}\rangle|^2 f(J', J''), \quad (1)$$

where $Q(R)$ is the quadrupole moment in atomic units, $E_{v'J'}$–$E_{v''J''}$ is the transition energy in atomic units, and $f(J', J'')$ is the branching ratio

$$f(J', J'') = \frac{(J' + 1)(J' + 2)}{(2J' + 1)(2J' + 3)} \quad (J'' = J' + 2)$$

$$= \frac{2J'(J' + 1)}{(2J' - 1)(2J' + 3)} \quad (J'' = J')$$

$$= \frac{J'(J' - 1)}{(2J' - 1)(2J' + 1)} \quad (J'' = J' - 2). \quad (2)$$

The wave functions $X_{vJ}(R)$ were obtained by numerical integration of the radial equation

$$\frac{d^2 X_{vJ}(R)}{dR^2} + \left[E_{vJ} - \frac{2\mu}{m} V(R) - \frac{J(J + 1)}{R^2}\right] X_{vJ}(R) = 0, \quad (3)$$

where μ is the reduced mass of H_2 and $V(R)$ is the interaction potential of the ground electronic $X\,^1\Sigma_g^+$ state of the molecule. Accurate values of $V(R)$ have been calculated by Kolos and Wolniewicz (1968) and of $Q(R)$ by Kolos and Wolniewicz (1965) and Dalgarno *et al.* (1969).

The radiative lifetime of the level vJ is

$$\tau_{vJ} = \left\{\sum_{v''} \sum_{J''} A(vJ, v''J'')\right\}^{-1} \text{s}. \quad (4)$$

Values of τ_{vJ} are given in Table 1. For $v \geq 1$, τ_{vJ} are usually of the order of 10^5–10^6 s. For $v = 0$, τ_{vJ} decreases as J^{-5}.

TABLE 1

LIFETIMES $\tau(vJ)$ OF THE ROTATION-VIBRATIONAL LEVELS OF H_2 IN UNITS OF 10^6 SECONDS

	J										
v	0	1	2	3	4	5	6	7	8	9	10
0	...	...	3.39(4)*	2.10(3)	3.63(2)	1.02(2)	37.9	17.0	8.75	4.99	3.09
1	1.17	1.17	1.18	1.20	1.22	1.26	1.31	1.36	1.40	1.44	1.38
2	0.612	0.612	0.614	0.618	0.628	0.644	0.668	0.698	0.735	0.794	0.815
3	0.422	0.422	0.426	0.422	0.425	0.433	0.446	0.464	0.488	0.532	0.557
4	0.328	0.327	0.325	0.324	0.326	0.329	0.337	0.349	0.365	0.398	0.418
5	0.270	0.269	0.268	0.266	0.266	0.268	0.273	0.282	0.294	0.321	0.338
6	0.234	0.233	0.231	0.230	0.229	0.231	0.234	0.241	0.251	0.275	0.289
7	0.211	0.210	0.209	0.207	0.206	0.207	0.211	0.216	0.225	0.248	0.262
8	0.198	0.197	0.196	0.194	0.194	0.195	0.198	0.204	0.213	0.237	0.251
9	0.194	0.193	0.192	0.191	0.191	0.192	0.196	0.203	0.213	0.239	0.255
10	0.199	0.199	0.198	0.197	0.198	0.200	0.206	0.214	0.227	0.259	0.282
11	0.217	0.217	0.217	0.217	0.219	0.224	0.233	0.246	0.266	0.312	0.352
12	0.259	0.259	0.260	0.263	0.269	0.280	0.298	0.326	0.370	0.467	0.597
13	0.360	0.363	0.370	0.383	0.405	0.444	0.512	0.645	0.836	1.42	2.75
14	0.777	0.807	0.881	1.05	1.30	1.76	2.44	3.57	5.68	1.1(2)	1.2(2)

* $3.39(4) \equiv 3.39 \times 10^4$.

TABLE 2

TRANSITION PROBABILITIES FOR EMISSION FROM vJ = 62, 65, AND 68 (in s^{-1})

v''	J''	$A(62, v''J'')$	J''	$A(65, v''J'')$	J''	$A(68, v''J'')$
6	0	1.30(−11)	3	4.03(−9)	6	4.05(−8)
5	0	1.92(−7)	3	1.82(−7)	6	2.51(−8)
	2	2.64(−7)	5	2.05(−7)	8	1.56(−7)
	4	3.02(−7)	7	1.10(−7)	10	2.93(−8)
4	0	8.27(−7)	3	1.43(−6)	6	1.31(−6)
	2	9.93(−7)	5	8.54(−7)	8	7.73(−7)
	4	9.82(−7)	7	4.06(−7)	10	1.64(−7)
3	0	2.75(−7)	3	6.82(−7)	6	8.99(−7)
	2	2.71(−7)	5	2.46(−7)	8	2.45(−7)
	4	1.31(−7)	7	1.51(−8)	10	2.20(−10)
2	0	4.17(−8)	3	1.49(−7)	6	2.54(−7)
	2	3.16(−8)	5	3.04(−8)	8	3.27(−8)
	4	2.52(−9)	7	2.99(−9)	10	1.19(−8)
1	0	3.21(−9)	3	1.61(−8)	6	3.35(−8)
	2	1.57(−9)	5	1.33(−9)	8	1.37(−9)
	4	4.14(−10)	7	3.27(−9)	10	5.40(−9)
0	0	3.43(−10)	3	2.11(−9)	6	4.97(−9)
	2	1.91(−10)	5	2.98(−10)	8	4.54(−10)
	4	3.07(−12)	7	3.56(−11)	10	3.16(−11)

The selection rules for quadrupole transitions are $J'-J'' = 0, \pm 2$, but there are no selection rules governing the changes in vibrational quantum numbers, and the cascading pattern is a complicated one. Because the transition frequency enters in the fifth power, the more energetic transitions tend to dominate the cascade, but cancellation effects in the evaluation of the matrix element of $Q(R)$ partly counteract this tendency. It is the case that transitions in which J decreases by 2 are generally more probable than the less energetic transitions in which J remains unchanged or increases by 2, although exceptions do occur.

An extract from the calculated transition probability array is reproduced in Table 2 which lists $A(62, v''J'')$, $A(65, v''J'')$, and $A(68, v''J'')$. The array shows that for $v' = 6$, the most probable decay path leads to $v'' = 4$, though both $v'' = 5$ and $v'' = 3$ are also significantly populated. Similar tables have been produced for all $v' \leq 14$ and $J \leq 10$.

For astrophysical applications, it is more useful to consider the equilibrium population $n(vJ)$ cm^{-3} of any level vJ produced by cascading from an initial level v_0J_0 which is assumed to be populated at a rate $Q(v_0J_0)$ cm^{-3} s^{-1}. Then

$$n(v_0J_0) = Q(v_0J_0)/A(v_0J_0) \tag{5}$$

and

$$n(vJ)A(vJ) = \sum_{v''=v}^{v_0} \sum_{J''=0}^{J_{\max}} n(v''J'')A(v''J'', vJ)\,. \tag{6}$$

We chose $J_{\max} = 10$ for the present calculation, which should be sufficient for most applications involving interstellar clouds. For each initial state (v_0J_0), the values of $n(vJ)A(vJ)$ may be evaluated directly beginning with $v = v_0$ and progressing downward to $v = 0$ for all possible J. For the larger values of v_0, pure rotational transitions are relatively unimportant compared with transitions in which $\Delta v \geq 1$. To study the population of levels $(v = 0, J)$, the entire cascade may be characterized by a set of cascade efficiency arrays for entry levels (v_0J_0)

$$a(v_0J_0; J) = n(v = 0, J)A(v = 0, J) \tag{7}$$

obtained from (6) for a given rate of entry into the cascade of $Q(v_0J_0) = 1.0$ cm^{-3} s^{-1}. The cascade is thus normalized so that

$$\sum_{J=0}^{J_{\max}} a(v_0J_0; J) = 1.0 \tag{8}$$

for every pair of v_0 and J_0. These cascade efficiencies are tabulated in Table 3. In practice, it was possible to achieve the normalization of (8) to within 1 percent by retaining only the most probable transitions out of each level. This reduces the number of transitions that must be considered to about 1840, a number which includes virtually all those for which $A(v'J', v''J'') \gtrsim 10^{-9}$ s^{-1}.

TABLE 3

CASCADE EFFICIENCY FACTORS $a(v_0 J_0; J)$

	J_0						J_0				
v_0	0	2	4	6	8	10	1	3	5	7	9
	$v = 0, J = 0$						$v = 0, J = 1$				
1.....	0.00000	0.29882	0.00095	0.00003	0.00000	0.00000	0.50387	0.41591	0.00484	0.00036	0.00009
2.....	0.23532	0.16126	0.10543	0.00193	0.00014	0.00003	0.47866	0.37971	0.15762	0.00717	0.00103
3.....	0.21318	0.14704	0.13201	0.02631	0.00141	0.00019	0.44606	0.37243	0.24235	0.04069	0.00428
4.....	0.16070	0.16287	0.12466	0.06126	0.00467	0.00046	0.42423	0.37691	0.27407	0.09929	0.01046
5.....	0.15332	0.16047	0.12625	0.08276	0.01431	0.00128	0.41031	0.37765	0.29416	0.15028	0.02466
6.....	0.16018	0.15247	0.13236	0.09295	0.02929	0.00276	0.40235	0.37608	0.30932	0.18701	0.04951
7.....	0.15968	0.14884	0.13584	0.09976	0.04371	0.00590	0.39637	0.37456	0.32063	0.21395	0.07800
8.....	0.15489	0.14831	0.13668	0.10560	0.05539	0.01076	0.39449	0.37346	0.32792	0.23428	0.10525
9.....	0.15112	0.14812	0.13694	0.11039	0.06431	0.01645	0.38809	0.37285	0.33345	0.25013	0.12870
10.....	0.14934	0.14735	0.13692	0.11391	0.07087	0.02190	0.38569	0.37194	0.33620	0.26154	0.14764
11.....	0.14846	0.14681	0.13699	0.11649	0.07592	0.02658	0.38357	0.37034	0.33960	0.27049	0.16173
12.....	0.14818	0.14584	0.13737	0.11784	0.07935	0.02971	0.38195	0.37039	0.34055	0.27625	0.17189
13.....	0.14768	0.14517	0.13708	0.12147	0.00000	0.00000	0.38105	0.36549	0.33960	0.27775	0.00000
14.....	0.14753	0.14370	0.13599	0.00000	0.00000	0.00000	0.37553	0.36277	0.34610	0.00000	0.00000
	$v = 0, J = 2$						$v = 0, J = 3$				
1.....	0.99953	0.35856	0.48915	0.01579	0.00232	0.00093	0.49637	0.33349	0.53575	0.03968	0.01045
2.....	0.49529	0.54273	0.39885	0.19151	0.01870	0.00456	0.42304	0.42274	0.43809	0.21386	0.04047
3.....	0.47643	0.53092	0.40035	0.29058	0.05428	0.00996	0.41982	0.43427	0.39565	0.33200	0.07751
4.....	0.53056	0.48589	0.43738	0.31659	0.12170	0.02032	0.42527	0.42367	0.40436	0.35547	0.14683
5.....	0.51775	0.47734	0.44874	0.33894	0.18205	0.03613	0.42574	0.41926	0.41004	0.36284	0.21748
6.....	0.49095	0.48206	0.44704	0.36293	0.22317	0.06367	0.42422	0.41989	0.41040	0.37067	0.26534
7.....	0.48088	0.48113	0.44672	0.38119	0.25330	0.09579	0.42287	0.41991	0.41021	0.37823	0.29711
8.....	0.48089	0.47658	0.44888	0.39294	0.27732	0.12646	0.42523	0.41952	0.41022	0.38258	0.31859
9.....	0.48115	0.47254	0.45146	0.40084	0.29647	0.15281	0.42166	0.41916	0.41101	0.38794	0.33248
10.....	0.47915	0.46979	0.45191	0.40575	0.31069	0.17349	0.42151	0.41836	0.40981	0.38951	0.34349
11.....	0.47615	0.46917	0.45160	0.41020	0.32211	0.18942	0.42095	0.41692	0.41098	0.39185	0.35006
12.....	0.47422	0.46743	0.45217	0.41165	0.32941	0.19888	0.42049	0.41726	0.40961	0.39274	0.35453
13.....	0.47205	0.46629	0.45058	0.42287	0.00000	0.00000	0.42032	0.41208	0.40694	0.39028	0.00000
14.....	0.47132	0.46221	0.44568	0.00000	0.00000	0.00000	0.41461	0.40949	0.41151	0.00000	0.00000
	$v = 0, J = 4$						$v = 0, J = 5$				
1.....	0.00000	0.34298	0.32614	0.56033	0.08219	0.03306	0.00000	0.24988	0.32488	0.56298	0.14820
2.....	0.27010	0.24662	0.35992	0.47206	0.22979	0.07159	0.09793	0.17074	0.30979	0.49665	0.25013
3.....	0.28118	0.26363	0.34481	0.39938	0.36142	0.11299	0.12539	0.16248	0.28184	0.40189	0.38791
4.....	0.25776	0.28724	0.31968	0.38100	0.38715	0.17090	0.13526	0.16862	0.24851	0.36162	0.41955
5.....	0.26930	0.29161	0.31111	0.36605	0.38528	0.24120	0.14389	0.17078	0.22823	0.33190	0.41360
6.....	0.28438	0.28934	0.31049	0.35156	0.37931	0.28984	0.15080	0.17080	0.21756	0.30668	0.39719
7.....	0.28974	0.29016	0.30934	0.34066	0.37312	0.32089	0.15556	0.17091	0.21049	0.28655	0.37861
8.....	0.28978	0.29253	0.30723	0.33385	0.36662	0.33916	0.15994	0.17151	0.20495	0.26970	0.36081
9.....	0.28993	0.29431	0.30568	0.32928	0.36062	0.34951	0.16121	0.17218	0.20100	0.25997	0.34377
10.....	0.29100	0.29491	0.30357	0.32499	0.35422	0.35439	0.16313	0.17240	0.19671	0.25034	0.33099
11.....	0.29197	0.29563	0.30232	0.32244	0.35101	0.35748	0.16442	0.17223	0.19504	0.24400	0.32079
12.....	0.29311	0.29527	0.30217	0.31844	0.34769	0.35684	0.16540	0.17268	0.19249	0.23890	0.31294
13.....	0.29332	0.29493	0.30075	0.32391	0.00000	0.00000	0.16609	0.17083	0.19005	0.23405	0.00000
14.....	0.29368	0.29278	0.29603	0.00000	0.00000	0.00000	0.16419	0.17018	0.18981	0.00000	0.00000
	$v = 0, J = 6$						$v = 0, J = 7$				
1.....	0.00000	0.00000	0.18388	0.32691	0.54319	0.21853	0.00000	0.00000	0.13442	0.32895	0.51764
2.....	0.00000	0.04978	0.12186	0.26973	0.50810	0.26288	0.00000	0.02639	0.08713	0.23950	0.51403
3.....	0.02953	0.05761	0.10764	0.23132	0.40105	0.38656	0.00783	0.02928	0.07252	0.19199	0.40251
4.....	0.05106	0.05956	0.10411	0.19595	0.34384	0.42213	0.01466	0.02852	0.06563	0.15649	0.33207
5.....	0.05733	0.06500	0.10000	0.17190	0.30179	0.41475	0.01848	0.02934	0.06042	0.13210	0.27627
6.....	0.06024	0.06986	0.09601	0.15683	0.26936	0.39325	0.02110	0.03037	0.05578	0.11589	0.23470
7.....	0.06428	0.07270	0.09365	0.14564	0.24386	0.36830	0.02318	0.03113	0.05241	0.10380	0.20269
8.....	0.06817	0.07432	0.09244	0.13711	0.22415	0.34443	0.02501	0.03163	0.04997	0.09386	0.17866
9.....	0.07098	0.07559	0.09169	0.13064	0.20940	0.32385	0.02613	0.03202	0.04820	0.08758	0.16212
10.....	0.07280	0.07664	0.09059	0.12509	0.19719	0.30589	0.02714	0.03227	0.04643	0.08156	0.14707
11.....	0.07395	0.07762	0.08985	0.12145	0.18912	0.29372	0.02787	0.03242	0.04554	0.07749	0.13789
12.....	0.07484	0.07817	0.08955	0.11765	0.18308	0.28321	0.02842	0.03265	0.04446	0.07435	0.13126
13.....	0.07535	0.07851	0.08890	0.11844	0.00000	0.00000	0.02880	0.03243	0.04359	0.07202	0.00000
14.....	0.07570	0.07826	0.08661	0.00000	0.00000	0.00000	0.02859	0.03244	0.04299	0.00000	0.00000

TABLE 3—*Continued*

	0	2	4	6	8	10	1	3	5	7	9
				$v = 0, J = 8$					$v = 0, J = 9$		
1.....	0.00000	0.00000	0.00000	0.09680	0.32656	0.45420	0.00000	0.00000	0.00000	0.06790	0.32358
2.....	0.00000	0.00000	0.01388	0.06145	0.21553	0.48411	0.00000	0.00000	0.00707	0.04253	0.19442
3.....	0.00000	0.00285	0.01489	0.04876	0.15989	0.38177	0.00000	0.00105	0.00739	0.03311	0.12778
4.....	0.00123	0.00501	0.01396	0.04204	0.12506	0.31114	0.00023	0.00179	0.00677	0.02698	0.09086
5.....	0.00324	0.00596	0.01380	0.03682	0.10186	0.25261	0.00062	0.00206	0.00653	0.02240	0.06765
6.....	0.00484	0.00667	0.01368	0.03300	0.08675	0.20948	0.00098	0.00223	0.00624	0.01926	0.05302
7.....	0.00577	0.00740	0.01348	0.03002	0.07553	0.17670	0.00126	0.00240	0.00595	0.01678	0.04305
8.....	0.00643	0.00803	0.01330	0.02783	0.06718	0.15230	0.00149	0.00253	0.00569	0.01479	0.03620
9.....	0.00702	0.00849	0.01316	0.02614	0.06094	0.13433	0.00168	0.00263	0.00547	0.01354	0.03214
10.....	0.00753	0.00884	0.01297	0.02464	0.05569	0.12084	0.00184	0.00270	0.00522	0.01235	0.02783
11.....	0.00793	0.00911	0.01286	0.02360	0.05215	0.11224	0.00196	0.00275	0.00509	0.01154	0.02554
12.....	0.00823	0.00929	0.01283	0.02249	0.04980	0.10568	0.00205	0.00279	0.00493	0.01091	0.02393
13.....	0.00843	0.00941	0.01273	0.02243	0.00000	0.00000	0.00212	0.00279	0.00481	0.01050	0.00000
14.....	0.00854	0.00944	0.01222	0.00000	0.00000	0.00000	0.00212	0.00281	0.00473	0.00000	0.00000
				$v = 0, J = 10$							
1.....	0.00000	0.00000	0.00000	0.00000	0.04574	0.29327					
2.....	0.00000	0.00000	0.00000	0.00341	0.02748	0.17647					
3.....	0.00000	0.00000	0.00037	0.00345	0.02182	0.10856					
4.....	0.00000	0.00006	0.00061	0.00314	0.01750	0.07491					
5.....	0.00002	0.00014	0.00069	0.00303	0.01406	0.05369					
6.....	0.00006	0.00022	0.00073	0.00285	0.01200	0.04085					
7.....	0.00013	0.00027	0.00078	0.00267	0.01024	0.03223					
8.....	0.00019	0.00032	0.00081	0.00252	0.00893	0.02643					
9.....	0.00024	0.00036	0.00083	0.00239	0.00799	0.02247					
10.....	0.00028	0.00040	0.00083	0.00225	0.00715	0.01960					
11.....	0.00032	0.00043	0.00084	0.00215	0.00657	0.01783					
12.....	0.00034	0.00045	0.00084	0.00204	0.00624	0.01653					
13.....	0.00036	0.00047	0.00084	0.00202	0.00000	0.00000					
14.....	0.00037	0.00048	0.00079	0.00000	0.00000	0.00000					

The rate of entry into level ($v = 0, J$) due to the cascade from excited levels and to direct entry from outside the cascade is

$$q_0(J) = \sum_{v'=1}^{14} \sum_{J'=0}^{10} Q(v'J')a(v'J'; J) + Q(0, J) . \tag{9}$$

A full treatment of the statistical equilibrium for the populations of the rotational levels of $v = 0$ must include all other processes which can redistribute the populations, such as rotationally inelastic collisions with atoms, other molecules, electrons, and protons (cf. Black and Dalgarno 1973), proton interchange reactions (Dalgarno *et al.* 1973), pure rotational transitions, and electronic excitation by ultraviolet photons. A detailed discussion of these problems will appear in a subsequent publication. Preliminary applications of Table 3 to the interpretation of the *Copernicus* data have been made by Black and Dalgarno (1973), Spitzer and Zweibel (1974), and Jura (1975).

b) Ultraviolet Absorption and Fluorescence

The processes which provide entry into the cascade are the ultraviolet absorption and fluorescence discussed above and the formation of new molecules initially in highly excited levels suggested by Spitzer and Cochran (1973) and discussed by Spitzer and Zweibel (1974). Photons of wavelength longer than the Lyman limit of atomic hydrogen, 912 Å, can be absorbed in the Lyman, $X\,^1\Sigma_g^+ \rightarrow B\,^1\Sigma_u^+$, and Werner, $X\,^1\Sigma_g^+ \rightarrow C\,^1\Pi_u$, systems of H_2. The population, $n^*(v'J')$, of a level $(v'J')$ of one of the excited electronic states is governed by

$$\sum_{v''} \sum_{j''} n(v''J'')R(v''J'', v'J') = n^*(v'J')A^*(v'J') , \tag{10}$$

where $n(v''J'')$ still refers to the population of a level in the ground state, and $A^*(v'J')$ is the total probability of radiative transitions out of level $(v'J')$ of the excited state to bound levels of $X\,^1\Sigma_g^+$ and to the vibrational continuum. The quantity $R(v''J'', v'J')$ is the rate of absorption in a particular line, l, where l stands for all the quantum numbers. Thus

$$R(v''J'', v'J') = \int_0^\infty \sigma_l(\nu)\phi(\nu)d\nu \ \mathrm{s}^{-1} , \tag{11}$$

where the quantity $\phi(\nu)$ is the ultraviolet flux at frequency ν in photons $cm^{-2}\ s^{-1}\ Hz^{-1}$ and $\sigma_l(\nu)$ is the photon absorption cross section in cm^2. The absorption cross section may be expressed in terms of the oscillator strength of transition l, f_l, and the Voigt profile function, $K(x, y)$,

$$\sigma_l(\nu) = \frac{0.012466}{\alpha_D} f_l K(x, y) . \tag{12}$$

The Voigt function depends upon the frequency relative to the line center, ν_0, in units of the Doppler half-width, α_D,

$$x = \frac{\nu - \nu_0}{\alpha_D} (\ln 2)^{1/2} ; \tag{13}$$

and also upon the ratio of natural line width to Doppler width,

$$y = \frac{A^*(v'J')}{\alpha_D} \frac{(\ln 2)^{1/2}}{4\pi} . \tag{14}$$

In this case,

$$K(x, y) = \frac{y}{\pi} \int_{-\infty}^{\infty} \frac{\exp(-t^2)}{y^2 + (x - t)^2} dt \tag{15}$$

with the normalization

$$\int_{-\infty}^{\infty} K(x, y) dx = \pi^{1/2} . \tag{16}$$

At the boundary of a cloud it should be valid to assume that the flux, $\phi(\nu)$, does not vary significantly across most lines and may therefore be taken outside the integral (11). Hence

$$R_l \approx \phi(\nu_0) \frac{\pi e^2}{mc} f_l . \tag{17}$$

A function of the form

$$\phi(\nu) = 2.0 \times 10^{-17} \lambda^3 I \text{ photons cm}^{-2}\ \text{s}^{-1}\ \text{Hz}^{-1} \tag{18}$$

has been chosen to represent the background interstellar radiation field for wavelengths $912 < \lambda < 1108$ Å. The quantity I is a scaling parameter such that for $I = 1.0$, $\phi(\nu)$ assumes a value at 1000 Å corresponding to a radiation energy density of 4×10^{-17} ergs cm^{-3} $Å^{-1}$ as suggested by Habing (1968). More recent measurements (Witt and Johnson 1973) and calculations (Jura 1974) of the strength of the interstellar radiation field suggest that values of $I = 1$–10 may be appropriate for typical regions. Equation (18) is intended to characterize an unattenuated radiation field at the boundary of a cloud. At greater depths into a cloud, the flux is reduced due to extinction by grains and absorption by atoms and molecules. An expression of the form of (18) reproduces the shape of the Witt and Johnson (1973) radiation field at longer wavelengths upon passage through a total hydrogen column density of at least 10^{20} cm^{-2}, given the canonical dust-gas ratio and a typical extinction curve in the ultraviolet (Bless and Savage 1972; York *et al.* 1973). The treatment of the radiative transfer for ultraviolet photons in an interstellar cloud and the computation of the absorption rates (11) as functions of depth for various model clouds are discussed in more detail elsewhere. Once the populations $n^*(v'J')$ are determined from (10), the cascade entry rates (8) are easily evaluated:

$$Q(v_0 J_0) = \sum_{v'} \sum_{J'} n^*(v'J') A^*(v'J', v_0 J_0) , \tag{19}$$

where $A^*(v'J', v_0 J_0)$ is the probability of a specific electronic transition. Dissociating transitions have been included implicitly through equation (10) since the relative probability, $\eta_{v'J'}$, with which level $(v'J')$ decays to the vibrational continuum of the ground state is given by

$$\eta_{v'J'} = \left[\sum_{v''} \sum_{J''} A^*(v'J', v''J'') \right] \Big/ [A^*(v'J')] . \tag{20}$$

Two examples of the cascade entry rates, one for a cloud boundary and the other for a column depth of hydrogen nuclei of 4×10^{20} cm^{-2}, are given in Table 4. The values are appropriate to $I = 10$ and a ratio of ortho-hydrogen to para-hydrogen of 1.20, and the populations are due to ultraviolet fluorescence and the subsequent cascade for the case in which only the initial levels $v = 0, J = 0, 1$ contribute to the excitation rates by ultraviolet pumping,

TABLE 4

CASCADE ENTRY RATES $Q(v_0J_0)$ cm^{-3} s^{-1} DUE TO ULTRAVIOLET PUMPING AT A CLOUD BOUNDARY AND AT A COLUMN DENSITY OF 5×10^{20} cm^{-2} FOR AN INCIDENT RADIATION FIELD $I = 10$

	Cloud Boundary				Cloud Center			
v_0	$J_0 = 0$	$J_0 = 1$	$J_0 = 2$	$J_0 = 3$	$J_0 = 0$	$J_0 = 1$	$J_0 = 2$	$J_0 = 3$
0.....	1.78−11	1.32−11	1.32−11	8.88−12	2.07−12	3.19−12	2.28−12	1.81−12
1.....	1.10−11	7.77−12	7.81−12	5.10−12	9.76−13	2.28−12	1.37−12	1.27−12
2.....	1.06−11	7.02−12	7.23−12	4.64−12	9.66−13	1.98−12	1.22−12	1.10−12
3.....	1.07−11	6.85−12	7.18−12	4.55−12	1.07−12	1.88−12	1.24−12	1.06−12
4.....	1.05−11	6.65−12	6.96−12	4.40−12	1.14−12	1.77−12	1.23−12	9.86−13
5.....	1.01−11	6.43−12	6.70−12	4.24−12	1.26−12	1.70−12	1.27−12	9.52−13
6.....	8.71−12	5.95−12	6.01−12	3.91−12	1.21−12	1.67−12	1.25−12	9.21−13
7.....	7.47−12	5.47−12	5.38−12	3.58−12	1.18−12	1.62−12	1.24−12	8.98−13
8.....	5.66−12	4.86−12	4.53−12	3.17−12	1.02−12	1.56−12	1.16−12	8.49−13
9.....	4.62−12	4.60−12	4.10−12	2.99−12	9.72−13	1.56−12	1.15−12	8.47−13
10.....	2.36−12	3.89−12	3.07−12	2.51−12	6.25−13	1.43−12	9.79−13	7.54−13
11.....	1.39−12	3.66−12	2.77−12	2.41−12	4.48−13	1.32−12	8.89−13	7.02−13
12.....	1.45−12	3.80−12	2.88−12	2.49−12	4.31−13	1.27−12	8.54−13	6.70−13
13.....	1.36−12	3.55−12	2.69−12	2.29−12	3.77−13	1.08−12	7.38−13	5.72−13
14.....	8.71−13	2.29−12	1.58−12	1.27−12	2.33−13	6.83−13	4.24−13	3.07−13

c) *Hot Molecule Formation*

Another process whereby excited rotation-vibration levels are populated is the formation of molecules upon grain surfaces. The formation of H_2 on grains has been discussed at length in the literature (Gould and Salpeter 1963; Knaap *et al.* 1966; Augason 1970; Hollenbach and Salpeter 1970, 1971; Lee 1972), but it is still uncertain how the binding energy of the molecule is distributed among the available degrees of freedom upon formation. For lack of better information, we assumed equipartition among the internal energy of the molecule, the kinetic energy of the molecule, and the internal energy of the grain lattice. We further assumed that the 1.5 eV of internal energy is distributed statistically among the rotation-vibration levels, so that the molecule is, in effect, formed at an effective temperature of about $T_f = 17400$ K. If $E(J)$ and $G(v)$ are the rotational and vibrational energies, then the efficiency, per molecule formation, with which a specific level (vJ) is populated is

$$P(vJ) = p_{\rm vib}(v)p_{\rm rot}(J)\,, \tag{21}$$

where

$$p_{\rm vib}(v) = c_v \exp\left(-G(v)/kT_f\right) \tag{22}$$

such that

$$\sum_{v=0}^{14} c_v \exp\left(-G(v)/kT_f\right) = 1.0 \tag{23}$$

and

$$p_{\rm rot}(J) = \frac{1}{4}\frac{(2J+1)\exp\left[-(E(J)-E(0))/kT_f\right]}{\sum_{\rm even\,J}(2J+1)\exp\left[-(E(J)-E(0))/kT_f\right]} \quad (\text{even } J)$$

$$= \frac{3}{4}\frac{(2J+1)\exp\left[-(E(J)-E(1))/kT_f\right]}{\sum_{\rm odd\,J}(2J+1)\exp\left[-(E(J)-E(1))/kT_f\right]} \quad (\text{odd } J)\,. \tag{24}$$

Cascade entry rates resulting from hot molecule formation are given in Table 5. They are appropriate to the same conditions as the results in Table 4, the rate of photodissociation being balanced by the rate of molecular formation.

As a process, hot molecule formation is usually more efficient than ultraviolet fluorescence in populating the very high rotational levels, but fluorescence tends to be more effective in interstellar clouds because fluorescence leading to bound states occurs between 5 and 10 times for each dissociation and hence in equilibrium for each molecule formed. At large depths into a cloud, ultraviolet photons are excluded and cosmic rays provide the main destruction of H_2. At such depths, the cascade is dominated by hot molecule formation.

III. THE INFRARED EMISSION SPECTRUM

Every transition in the rotation-vibration cascade gives rise to an infrared photon. In doing the cascade calculation, the equilibrium level populations, $n(vJ)$, are computed, so that the infrared line emissivities,

$$\epsilon(v'J', v''J'') = n(v'J')A(v'J', v''J'') \text{ photons cm}^{-3}\text{ s}^{-1}\,, \tag{25}$$

TABLE 5

CASCADE ENTRY RATES $Q(v_0J_0)$ cm^{-3} s^{-1} RESULTING FROM HOT MOLECULE FORMATION ON THE BOUNDARY OF A CLOUD OF DENSITY 10^3 cm^{-3} SUBJECTED TO AN ULTRAVIOLET RADIATION FIELD WITH $I = 10$

	J_0										
v_0	0	1	2	3	4	5	6	7	8	9	10
0.....	1.12−14	1.14−13	5.41−12	2.53−13	9.08−14	3.66−13	1.19−13	4.43−13	1.36−13	4.83−13	1.42−13
1.....	7.91−15	8.09−14	3.84−14	1.80−13	6.46−14	2.59−13	8.43−14	3.14−13	9.60−14	3.43−13	1.01−13
2.....	5.73−15	5.86−14	2.78−14	1.30−13	4.68−14	1.88−13	6.09−14	2.27−13	6.95−14	2.47−13	7.29−14
3.....	4.21−15	4.31−14	2.05−14	9.60−14	3.44−14	1.38−13	4.49−14	1.67−13	5.12−14	1.83−13	5.37−14
4.....	3.17−15	3.24−14	1.54−14	7.19−14	2.59−14	1.04−13	3.36−14	1.25−13	3.85−14	1.37−13	4.03−14
5.....	2.42−15	2.47−14	1.18−14	5.50−14	1.98−14	7.94−14	2.58−14	9.60−14	2.94−14	1.05−13	3.09−14
6.....	1.89−15	1.93−14	9.17−15	4.29−14	1.54−14	6.18−14	2.01−14	7.48−14	2.29−14	8.16−14	2.40−14
7.....	1.50−15	1.53−14	7.27−15	3.41−14	1.23−14	4.91−14	1.59−14	5.95−14	1.83−14	6.49−14	1.91−14
8.....	1.22−15	1.25−14	5.90−15	2.76−14	9.95−15	3.99−14	1.30−14	4.83−14	1.48−14	5.26−15	1.55−14
9.....	1.00−15	1.03−14	4.88−15	2.28−14	8.22−15	3.30−14	1.07−14	3.99−14	1.22−14	4.35−14	1.28−14
10.....	8.50−16	8.74−15	4.13−15	1.93−14	6.95−15	2.79−14	9.08−15	3.37−14	1.03−14	3.68−14	1.08−14
11.....	7.37−16	7.53−15	3.57−15	1.68−14	6.02−15	2.41−14	7.85−15	2.92−14	9.00−15	3.18−14	9.43−15
12.....	6.55−16	6.70−15	3.18−15	1.49−14	5.35−15	2.15−14	6.97−15	2.60−14	7.97−15	2.84−14	8.35−15
13.....	6.01−16	6.15−15	2.92−15	1.37−14	4.91−15	1.97−14	6.40−15	2.39−14	7.31−15	2.60−14	7.66−15
14.....	5.70−16	5.84−15	2.77−15	1.30−14	4.66−15	1.87−14	6.07−15	2.27−14	6.94−15	2.47−14	7.27−15

follow directly. Calculation of the intensity in a line,

$$I(v'J', v''J'') = \frac{1}{4\pi}\int \epsilon(v'J', v''J'')dx \text{ photons cm}^{-2}\text{ s}^{-1}\text{ sr}^{-1}, \quad (26)$$

involves an integration over the path through the cloud and thus requires a model for the depth-dependence of the level populations. Two competing effects occur: the excitation rates decrease with depth into a cloud as the ultraviolet absorption lines become increasingly opaque, but on the other hand the total molecular concentration increases as the dissociation rate decreases. In fact, for reasonable densities and boundary radiation fields, the two effects nearly cancel, as illustrated in Figure 1, in which the emissivities for several of the emission lines are shown to remain unchanged by more than a factor of 2 over substantial column depths. The results in Figure 1 apply to a cloud of constant total density $n = n(\text{H}) + 2n(\text{H}_2) = 1000$ cm^{-3}, temperature $T = 100$ K, and $I = 10$. At some point, hydrogen approaches complete conversion to molecular form while the ultraviolet excitation rate continues to decrease rapidly, with the result that the line emissivities drop until they reach the limit set by the hot molecule formation contribution in balance with cosmic-ray destructions.

In the model calculation described above, vibrationally excited molecules constitute a small fraction of the density. The depth-dependence of the concentrations in three of the excited states is illustrated in Figure 2. The

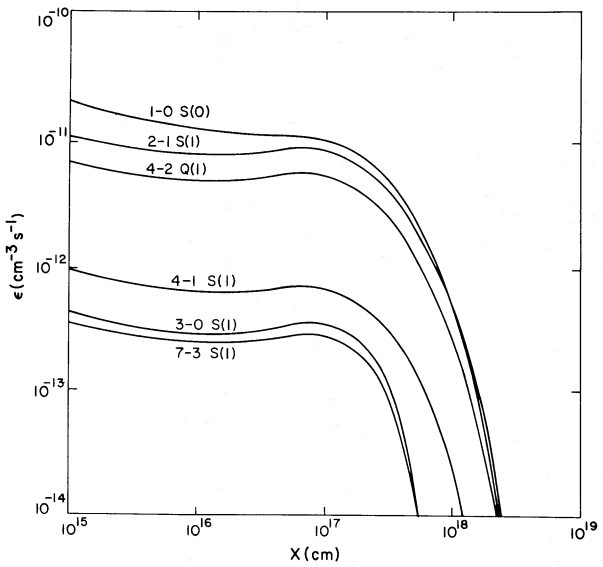

FIG. 1.—The emissivities ϵ in photons cm^{-3} s^{-1} for various lines of H_2 as a function of depth X into a cloud of hydrogen density 10^3 cm^{-3}.

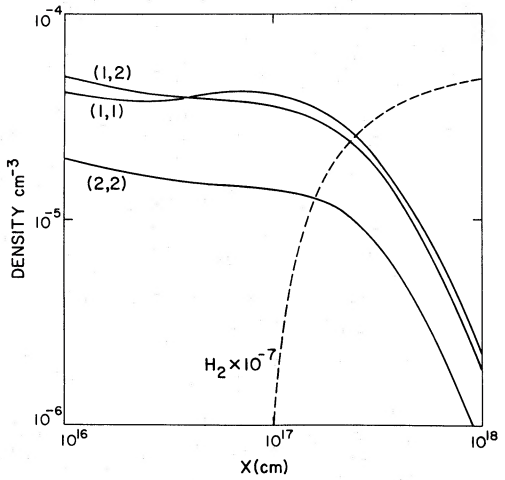

FIG. 2.—The equilibrium concentrations of rotational-vibrational levels vJ of H_2 as a function of depth X into a cloud of hydrogen density 10^3 cm^{-3}.

vibrationally excited molecules are confined to the outer parts of the cloud where the ultraviolet excitation rate is highest. When integrated over a path length which corresponds to a visual extinction of 0.5 mag, the abundance of molecules in all rotational levels of $v = 1$ is about the same as the abundance of molecules in the $v = 0$, $J = 7$ level and equals 6.5×10^{-6} times the total H_2 column density.

Tables 6 and 7 contain the predicted intensities for the model cloud described above with a total linear dimension of 10^{18} cm. The intensities of the very strongest lines produced in the cascade are given in photons cm^{-2} s^{-1} sr^{-1} and as fractions of the total ultraviolet fluorescence rate. The strongest lines in the near infrared at wavelengths less than 1.0 μ are presented in Table 7. The near-infrared lines tend to be less intense by factors of 50 or more than the strongest lines; however, detectors in the near-infrared can be more sensitive than those which operate at about 2 μ by a comparable factor. The total yield of the cascade is about three infrared photons emitted for each ultraviolet photon absorbed. The predicted line intensities for such a cloud are comparable to the present detection thresholds. A denser region exposed to a more intense radiation field will produce stronger infrared emission lines.

Since the intensity of H_2 emission depends upon the ultraviolet absorption rate and since the ultraviolet photons have a limited depth of penetration, only the outer edge of an externally illuminated cloud will contribute to the H_2 emission. As a result, the most favorable locations to search for the H_2 lines may be the edges of dense clouds near visible hot stars or dense neutral condensations embedded in emission nebulae.

TABLE 6

INTENSITIES OF THE 10 STRONGEST LINES IN THE CASCADE AND OF SEVERAL OTHER STRONG LINES IN UNITS OF 10^5 PHOTONS cm^{-2} s^{-1} sr^{-1} FOR A CLOUD OF DENSITY 1000 cm^{-3} AND LINEAR DIMENSION 10^{18} cm

Transition	Wavelength (μ)	I (10^5 photons cm^{-2} s^{-1} sr^{-1})	$I_{relative}$*
1–0 $Q(1)$.....	2.407	9.29	0.0252
1–0 $O(3)$.....	2.803	9.16	0.0248
1–0 $S(1)$.....	2.122	7.68	0.0208
1–0 $O(2)$.....	2.627	6.78	0.0184
1–0 $Q(2)$.....	2.413	6.30	0.0171
1–0 $Q(3)$.....	2.424	6.16	0.0167
1–0 $O(4)$.....	3.004	6.03	0.0163
2–1 $O(3)$.....	2.974	5.58	0.0151
2–1 $Q(1)$.....	2.551	5.56	0.0151
1–0 $S(0)$.....	2.223	5.17	0.0140
2–1 $S(1)$.....	2.248	4.23	0.0115
3–2 $Q(1)$.....	2.710	3.32	0.0090
4–2 $Q(1)$.....	1.398	2.59	0.0070
5–3 $Q(1)$.....	1.493	2.41	0.0065
3–1 $Q(1)$.....	1.314	1.77	0.0048

* $I_{relative}$ is the intensity expressed as a fraction of the total ultraviolet fluorescence rate.

TABLE 7

INTENSITIES OF SELECTED LINES HAVING WAVELENGTHS LESS THAN 1.0 MICRONS IN UNITS OF 10^4 PHOTONS cm^{-2} s^{-1} sr^{-1} FOR A CLOUD OF DENSITY 10^3 cm^{-3} AND DIMENSION 10^{18} cm

Transition	Wavelength (μ)	I (10^4 photons cm^{-2} s^{-1} sr^{-1})	$I_{relative}$*
5–2 $Q(1)$.....	0.9627	4.48	0.00121
5–2 $S(1)$.....	0.9232	4.65	0.00126
4–1 $S(1)$.....	0.9032	3.30	0.000894
11–6 $Q(1)$.....	0.8812	0.66	0.000179
3–0 $Q(1)$.....	0.8500	1.21	0.000328
4–1 $S(3)$.....	0.8462	1.82	0.000493
8–4 $S(1)$.....	0.8394	1.54	0.000417
3–0 $S(1)$.....	0.8153	1.59	0.000431
7–3 $S(1)$.....	0.7771	1.30	0.000352
6–2 $S(1)$.....	0.7240	0.92	0.000249

* $I_{relative}$ is the intensity expressed as a fraction of the total ultraviolet fluorescence rate.

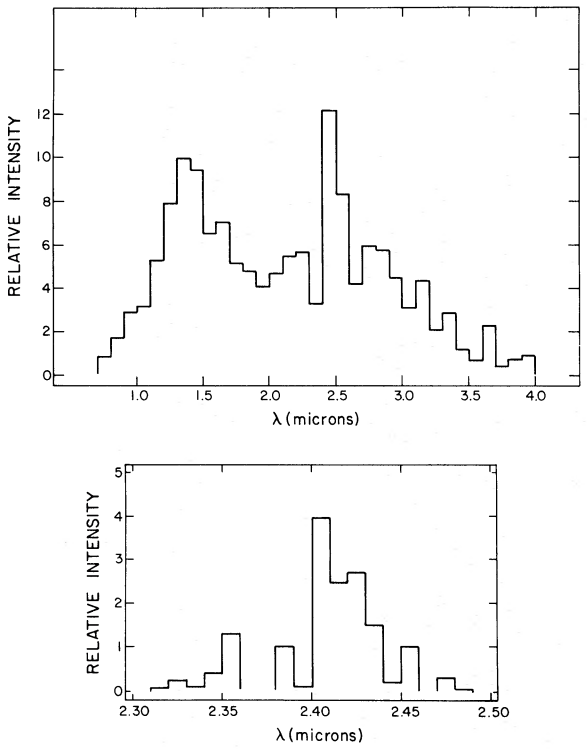

FIG. 3.—Dependence of the infrared response of H_2 on wavelength for bands of width 0.1 μ between 0.7 and 4.0 μ and of width 0.01 μ between 2.30 and 2.50 μ.

The distribution of the strongest lines with wavelength is such that there exists a large contrast in intensity between adjacent narrow bands around 2.4 μ. This feature is illustrated in Figure 3, which shows the spectrum of the model cloud between 0.7 and 4.0 μ wavelength in bands of 0.1 μ width and between 2.30 and 2.50 μ in bands 0.01 μ wide. The intensity in a band between 2.40 and 2.45 μ is about 4 times larger than in the adjacent band 2.35–2.40 μ. If this contrast could be detected above any continuum which might be present, it would provide a means of detecting H_2 with narrow-band filter photometry. However, an obvious observational difficulty occurs because the adjacent low-intensity band, 2.45–2.50 μ, lies at the edge of the atmospheric window, and the shorter-wavelength bands may not be free from atmospheric features.

We are greatly indebted to Dr. A. Timothy and to Dr. A. C. Allison for their early contributions to the calculation of the quadrupole emission transition probabilities. Our study of the cascading problem was intensified by the interest expressed by Dr. L. Spitzer.

REFERENCES

Augason, G. C. 1970, *Ap. J.*, **162**, 463.
Black, J. H., and Dalgarno, A. 1973, *Ap. J.* (*Letters*), **184**, L101.
Bless, R. C., and Savage, B. D. 1972, *Ap. J.*, **171**, 293.
Carruthers, G. R. 1970, *Ap. J.* (*Letters*), **161**, L81.
Dalgarno, A., Allison, A. C., and Browne, J. C. 1969, *J. Atmos. Sci.*, **26**, 946.
Dalgarno, A., Black, J. H., and Weisheit, J. C. 1973, *Ap. Letters*, **14**, 77.
Dalgarno, A., and Stephens, T. L. 1970, *Ap. J.* (*Letters*), **160**, L107.
Dalgarno, A., and Wright, E. L. 1972, *Ap. J.* (*Letters*), **174**, L49.
Field, G. B., Somerville, W. B., and Dressler, K. 1966, *Ann. Rev. Astr. and Ap.*, **4**, 207.
Gould, R. J., and Harwit, M. 1963, *Ap. J.*, **137**, 694.
Gould, R. J., and Salpeter, E. E. 1963, *Ap. J.*, **138**, 393.
Gull, T. R., and Harwit, M. 1971, *Ap. J.*, **168**, 15.
Habing, H. J. 1968, *B.A.N.*, **19**, 421.
Hollenbach, D. J., and Salpeter, E. E. 1970, *J. Chem. Phys.*, **53**, 79.
———. 1971, *Ap. J.*, **163**, 155.
Hollenbach, D. J., Werner, M. W., and Salpeter, E. E. 1971, *Ap. J.*, **163**, 165.
Jura, M. 1974, *Ap. J.*, **191**, 375.
———. 1975, *ibid.*, **197**, 575 and 581.
Kolos, W., and Wolniewicz, L. 1965, *J. Chem. Phys.*, **43**, 2429.
———. 1968, *J. Chem. Phys.*, **48**, 404.
Knaap, H. F. P., van den Meydenberg, C. J. N., Beenakker, M. J. M., and van de Hulst, H. C. 1966, *B.A.N.*, **18**, 256.
Lee, T. J. 1972, *Nature*, **237**, 99.
Nishimura, S., and Takayanagi, K. 1969, *Pub. Astr. Soc. Japan*, **21**, 111.
Smith, A. M. 1973, *Ap. J.* (*Letters*), **179**, L11.
Solomon, P. M., and Werner, M. W. 1971, *Ap. J.*, **165**, 41.
Spitzer, L., and Cochran, W. D. 1973, *Ap. J.* (*Letters*), **186**, L23.
Spitzer, L., Cochran, W. D., and Hirshfeld, A. 1974, *Ap. J. Suppl.*, **28**, 373.
Spitzer, L., Drake, J. F., Jenkins, E. B., Morton, D. C., Rogerson, J. B., and York, D. G. 1973, *Ap. J.* (*Letters*), **181**, L116.
Spitzer, L., and Zweibel, E. G. 1974, *Ap. J.* (*Letters*), **191**, L127.
Stecher, T. P., and Williams, D. A. 1967, *Ap. J.* (*Letters*), **149**, L29.
Werner, M. W., and Harwit, M. 1968, *Ap. J.*, **154**, 881.
Witt, A. N., and Johnson, M. W. 1973, *Ap. J.*, **181**, 363.
York, D. G., Drake, J. F., Jenkins, E. B., Morton, D. C., Rogerson, J. B., and Spitzer, L. 1973, *Ap. J.* (*Letters*), **182**, L1.

J. H. BLACK: School of Physics and Astronomy, University of Minnesota, Minneapolis, MN 55455

A. DALGARNO: Center for Astrophysics, 60 Garden St., Cambridge, MA 02138